

Molecular gas in blue compact dwarf galaxies

L.T. Barone ^{★ 1,2}, A. Heithausen¹, S. Hüttemeister¹, T. Fritz¹ and U. Klein¹

¹*Radioastronomisches Institut der Universität Bonn, Auf dem Hügel 71, D-53121 Bonn, Germany*

²*Dipartimento di Astronomia, Università degli Studi di Bologna, Bologna, Italy.*

Accepted Received

ABSTRACT

Blue compact dwarf galaxies (BCDGs) are currently undergoing strong bursts of star formation. Nevertheless, only a few of them have been clearly detected in CO, which is thought to trace the “fuel” of star formation: H₂. In this paper we present a deep search for CO $J = 1 \rightarrow 0$ and $J = 2 \rightarrow 1$ emission lines in a sample of 8 BCDGs and two companions. Only 2 of them (Haro 2 and UM 465) are detected. For the other galaxies we have obtained more stringent upper limits on the CO luminosity than published values. We could not confirm the previously reported “detection” of CO for the galaxies UM 456 and UM 462. We analyze a possible relation between metallicity, CO luminosity, and absolute blue magnitude of the galaxies. We use previously determined relations between $X \equiv N(\text{H}_2)/I_{\text{CO}}$ and the metallicity to derive molecular cloud masses or upper limits for them. With these “global” X_{CO} -values we find that for those galaxies which we detect in CO, the molecular gas mass is similar to the HI mass, whereas for the non-detections, the upper limits on the molecular gas masses are significantly lower than the HI mass. Using an LVG (Large Velocity Gradient) model we show that X_{CO} depends not only on metallicity but also on other physical parameters such as, volume density and kinetic temperature, which rises the question on the validity of “global” X_{CO} -factors.

Key words: Galaxies: dwarf – galaxies: ISM – galaxies: starburst – radio lines: ISM

1 INTRODUCTION

A particular class of dwarf galaxies named Blue Compact Dwarf Galaxies (BCDGs, Sargent & Searle, (1970)) has seen increasing interest among astrophysicists because of their extreme current star forming activity which is in contrast to their apparent “youth” in terms of chemical evolution. BCDGs represent about 5% of all dwarfs (Salzer 1989), (Sage et al., 1992) and are among the smallest star forming galactic systems known.

One of their outstanding properties is that their optical spectra are dominated by lines characteristic of HII regions, which is the reason why they are frequently termed “HII galaxies”. From optical spectroscopy we know that many HII galaxies have low heavy element abundances, typically down by a factor of three up to more than twenty compared to the solar neighbourhood (Kunth & Östlin, 2000).

It quickly became clear that these objects must form stars in what is called a burst, otherwise the observed star formation rate would be in conflict with their total gas masses as derived from HI observations (Thuan & Martin,

1981). Such a burst may last some 10^8 yrs, with a time span between bursts of the order of 10^9 yrs. It has been suggested that interaction with companions might trigger their star formation (Brinks, 1990), but Taylor et al. (1995) found that only about 60% of HII galaxies have companions, often with masses about $\frac{1}{10}$ of the main galaxy.

One of the most interesting and important issues which has not been settled so far is the molecular gas content of these galaxies. Molecular hydrogen is believed to be the preponderant seed for star formation, so it is a natural assumption that large amounts of H₂ should be present in BCDGs. Yet the results have been anything but conclusive so far. Following early attempts to detect the CO line in BCDGs (Tacconi & Young, 1984), there have been a number of observations to confirm or reject those inconclusive measurements (e.g. Sage et al. (1992), hereafter SSLH; Gondhalekar et al. (1998); Taylor, Kobulnicky & Skillman (1998), hereafter TKS). Surprisingly, the results remained partially contradictory, as for instance in the case of II Zw 40 (Arnault et al. (1988); SSLH), although improved instrumentation had been involved.

Prompted by the difficulty to detect the CO line – relied upon as a good tracer of molecular hydrogen content – in BCDGs, some of the pertinent publications prematurely

[★] *Present address:* Osservatorio Astronomico di Brera-Merate, Via Bianchi 46, I-23807 Merate (LC), Italy.

Table 1. Properties of the galaxies and final observational results.

Galaxy	α (1950)	δ (1950)	Distance Mpc	Abundance 12+log O/H	v_{hel} [km s ⁻¹]	Δv [km s ⁻¹]	rms (1 σ) [mK]	I_{CO} [K km s ⁻¹]	L_{CO} [10 ⁶ K km s ⁻¹ pc ²]
UM 422	11 17 37	+02 48 16	21.3	8.03	1600	–	3.6	< 0.21	< 4.24
					1600	–	7.5	< 0.42	< 2.76
UM 439	11 34 02	+01 05 38	14.7	8.03	1097	–	4.6	< 0.27	< 1.83
					1097	–	11.6	< 0.64	< 1.56
UM 446	11 39 02	-01 37 26	24.0	–	1792	–	21.9	< 0.43	< 2.22
					1792	–	44.7	< 2.47	< 4.01
UM 452	11 44 26	-00 00 57	19.2	–	1439	–	7.7	< 0.44	< 1.47
					1439	–	11.6	< 0.64	< 0.69
UM 456	11 48 01	-00 17 23	23.3	7.89	1749	–	4.3	< 0.25	< 3.85
					1749	–	8.7	< 0.47	< 2.78
UM 456A	11 48 00	-00 15 30	23.3	–	1749	–	14.5	< 0.85	< 4.14
					1749	–	27.1	< 1.49	< 2.33
UM 456B	11 47 53	-00 17 00	23.3	–	1749	–	9.1	< 0.52	< 2.55
					1749	–	18.2	< 1.00	< 1.55
UM 462	11 50 13	-02 11 26	13.9	7.97	1051	–	7.8	< 0.46	< 0.79
					1051	–	14.4	< 0.80	< 0.44
UM 465	11 51 38	+00 24 56	15.4	8.57	1144	17±2	7.8	0.64±0.07	3.12±0.32 ^b
					1144	35±13	18.8	1.47±0.35	2.91±0.71 ^b
Haro 2 ^a	10 29 22	+54 39 24	20.5	8.4	1401	19±8	9.3	4.2±0.4	36.7±3.5 ^b
					1452	70.0			
					1401	18±20	14.0	6.44±1.33	22.7±4.7 ^b
					1452	70.0			

Remarks: First line for each galaxy refers to the ($J = 1 \rightarrow 0$) transition, second line to the ($2 \rightarrow 1$) transition. 3 σ upper limits to I_{CO} are obtained with $\Delta v = 70$ km s⁻¹. The distances are taken from Taylor et al. (1998) for most of the UM galaxies and from Loose & Thuan (1986) for Haro 2. The distance of UM 446 was obtained for a Hubble flow with $H_0 = 75$ km s⁻¹ Mpc⁻¹. The velocities indicated in Column 7 are derived from HI widths for the non-detections. Metallicities are taken from Campos-Aguilar, Moles & Masegosa (1993) for UM galaxies, who give a general uncertainty for the values of better than 0.1 dex, and from Sage et al. (1992) for Haro 2. *a*: Two components found. *b*: Errors include only statistical errors, not systematic ones.

concluded that molecular gas is deficient in these systems. However, part of the difficulties to detect CO might have been due to beam filling and sensitivity problems. Taking e.g. 30 Dor in the LMC as a template giant star-forming complex, it is clear that, if placed at some larger distance and covered by the beam, it could have escaped detection, as CO brightness is rather low there, due to strong photodissociation in the high interstellar radiation field (Cohen et al., 1988). The same might be true for BCDGs. In this case, high-sensitivity mapping might reveal previously undetected CO emission.

We have therefore conducted a search for CO in gas-rich (based on HI) HII galaxies, using the IRAM 30m telescope. In contrast to previous projects (e.g. SSLH, Gondhalekar et al. (1998)), our observations not only consisted of single pointings towards the brightest position in the galaxies, but involved mapping a number of positions in them, to detect possible gas concentrations away from photodissociation regions. Obtaining sensitive upper limits to the CO luminosity in these systems is as much a goal of this study as detecting emission.

In Section 2 we present details of our observations. In Section 3 we present our data, and compare it with previous results. In the subsequent section (Sec. 4) we discuss possible causes for the detections and non-detections. This section is

divided into three subsections: Section 4.1 deals with the physical conditions of the gas derived from a LVG model; in Section 4.2 we analyze the relationship between metallicity and CO luminosity; finally, in Section 4.3 we discuss the X_{CO} factor problem, which has been heatedly debated in the past years and has not yet found a clear resolution. Our conclusions are presented in the last section (Sec. 5).

2 OBSERVATIONS

The CO observations were carried out in October 1996 with the IRAM 30m Telescope on Pico Veleta in Spain. Our target galaxies – except Haro 2 – have been selected from the sample examined by (Taylor et al., 1995) in the 21 cm line of atomic hydrogen. Pointing positions were chosen from peak HI column densities, as seen in their high angular resolution VLA observations. The basic properties of the galaxies are listed in Table 1. In the $J = 1 \rightarrow 0$ transition (115 GHz) the HPBW is 22'', whilst in the $J = 2 \rightarrow 1$ transition (230 GHz) it is 12.''5. At the distance of the galaxies, 14.7 Mpc to 23.3 Mpc, the beam size at 115 GHz corresponds to 1.6 kpc to 2.5 kpc.

Two independent SIS receivers have been used simultaneously at each frequency. More than 90% of our observations had $T_{sys} \leq 600$ K both at 230 and at 115 GHz.

Table 2. Observed positions

Source	$\Delta\alpha^a$ [$''$]	$\Delta\delta^a$ [$''$]	Transition	rms [mK]
UM 422	0	0	$^{12}\text{CO}(1-0)$	7
			$^{12}\text{CO}(2-1)$	18
	-20	20	$^{12}\text{CO}(1-0)$	7
			$^{12}\text{CO}(2-1)$	13
	20,	0	$^{12}\text{CO}(1-0)$	8
			$^{12}\text{CO}(2-1)$	22
	-20	0	$^{12}\text{CO}(1-0)$	4
			$^{12}\text{CO}(2-1)$	4
	0	20	$^{12}\text{CO}(1-0)$	3
			$^{12}\text{CO}(2-1)$	9
UM 439	0	0	$^{12}\text{CO}(1-0)$	5
			$^{12}\text{CO}(2-1)$	18
	10	-20	$^{12}\text{CO}(1-0)$	5
			$^{12}\text{CO}(2-1)$	13
	-10	20	$^{12}\text{CO}(1-0)$	7
			$^{12}\text{CO}(2-1)$	20
	10	0	$^{12}\text{CO}(1-0)$	7
			$^{12}\text{CO}(2-1)$	9
UM 446	0	0	$^{12}\text{CO}(1-0)$	16
			$^{12}\text{CO}(2-1)$	22
UM 452	0	5	$^{12}\text{CO}(1-0)$	5
			$^{12}\text{CO}(2-1)$	7
UM 456	0	0	$^{12}\text{CO}(1-0)$	8
			$^{12}\text{CO}(2-1)$	13
	10	10	$^{12}\text{CO}(1-0)$	5
			$^{12}\text{CO}(2-1)$	9
	10	0	$^{12}\text{CO}(1-0)$	4
			$^{12}\text{CO}(2-1)$	9
	20	20	$^{12}\text{CO}(1-0)$	7
			$^{12}\text{CO}(2-1)$	11
UM 456 A	5	-5	$^{12}\text{CO}(1-0)$	11
			$^{12}\text{CO}(2-1)$	13
UM 456 B	0	0	$^{12}\text{CO}(1-0)$	7
			$^{12}\text{CO}(2-1)$	11
UM 462	10	5	$^{12}\text{CO}(1-0)$	5
			$^{12}\text{CO}(2-1)$	11
UM 465	2	0	$^{12}\text{CO}(1-0)$	4
			$^{12}\text{CO}(2-1)$	8
	-18	10	$^{12}\text{CO}(1-0)$	4
			$^{12}\text{CO}(2-1)$	9
	-8	10	$^{12}\text{CO}(1-0)$	7
			$^{12}\text{CO}(2-1)$	11
Haro 2	0	0	$^{12}\text{CO}(1-0)$	18
			$^{12}\text{CO}(2-1)$	24
	10	0	$^{12}\text{CO}(1-0)$	20
			$^{12}\text{CO}(2-1)$	31
	0	10	$^{12}\text{CO}(1-0)$	19
			$^{12}\text{CO}(2-1)$	33

Remarks: a : Offsets are relative to positions in Table 1.

An autocorrelator with a spectral resolution of 0.625 MHz at 115 MHz and 1.25 MHz at 230 MHz and a filter spectrometer with 1 MHz resolution were used. A baseline of zeroth or first order was always subtracted, and the spectra were summed up to improve the signal-to-noise ratio; the spectra were finally smoothed to roughly the same velocity resolution (5.2 km s^{-1} for the $J = 1 \rightarrow 0$ and 4.8

Table 3. Fit results for every position in Haro 2 and UM 465.

Galaxy	$\Delta\alpha$ [$''$]	$\Delta\delta$ [$''$]	I_{CO} [K km s $^{-1}$]	v_{hel} [km s $^{-1}$]	Δv [km s $^{-1}$]
Haro 2	00	00	3.8 ± 0.3	1452 ± 2	61 ± 4
			6.2 ± 0.4	1455 ± 2	85 ± 5
	10	00	3.9 ± 0.4	1441 ± 4	73 ± 8
			3.7 ± 0.7	1443 ± 6	64 ± 11
	00	10	4.2 ± 0.2	1445 ± 2	71 ± 4
			7.6 ± 0.3	1446 ± 2	80 ± 4
UM 465	-08	10	0.64 ± 0.13	1143 ± 2	20 ± 6
			0.95 ± 0.13	1147 ± 1	19 ± 4
	02	00	0.31 ± 0.07	1144 ± 1	14 ± 3
			0.60 ± 0.07	1140 ± 6	43 ± 11
	-18	10	0.75 ± 0.15	1153 ± 6	67 ± 9
			no line		

Remarks: First line for each galaxy and position refers to the ($J = 1 \rightarrow 0$) transition, second line to the ($2 \rightarrow 1$) transition.

km s^{-1} for the $J = 2 \rightarrow 1$ transition). Spectra were obtained with a wobbling secondary mirror with a wobbler throw of $\pm 4'$ in azimuth. All temperatures throughout this article refer to main beam brightness with T_{mb} derived using $\eta_{\text{mb}}(115) = 0.74$ and $\eta_{\text{mb}}(230) = 0.45$.

3 RESULTS

Table 1 gives an overview of the observed galaxies and some of their known properties, and lists results of the galaxy-averaged CO spectra. We mapped most of the galaxies in our sample in order to cover most of the area where emission (perhaps in “hot spots”) might be present, and obtained low rms noise levels. Nevertheless, we detected CO only in Haro 2 and in UM 465. For all the other galaxies we obtained low upper limits. It is interesting to note that the SMC, with an H_2 mass of $3 \cdot 10^7 \text{ M}_{\odot}$ would be just detectable with our sensitivity if placed at a distance of 15 Mpc.

In Table 2, all positions observed in all galaxies are listed, with the final rms obtained for single positions. In Fig. 1 and 3, the $J = 1 \rightarrow 0$ maps of Haro 2 and UM 465 are displayed.

In Table 1 we also give a summary of our results. For the detections, we give the parameters of a Gaussian fit which we obtained for the lines averaged over all positions. In all other cases, upper limits to the CO intensity were calculated, again based on the average of *all* positions. These upper limits were derived as $I_{\text{CO}} \leq \sigma \Delta v_{\text{ch}} \sqrt{N}$, where σ is the rms noise level obtained in the baseline range, Δv_{ch} is the velocity width of each channel and N is the number of channels involved. We always assumed a total line width of 70 km s^{-1} , as this is the average velocity width one would expect from the CO detections in the literature (see for example SSLH and Gondhalekar et al. (1998)). In the case of detections, I_{CO} has been calculated based on Gaussian fits to the spectra. Based on the I_{CO} values, CO luminosities (L_{CO}) were calculated. Those for UM 465 and Haro 2 are lower limits, because we did not completely map the CO gas. The other values are upper limits for the galaxies.

In the following sections we summarize briefly our main results for the individual galaxies in comparison to previously published data where applicable. We also give

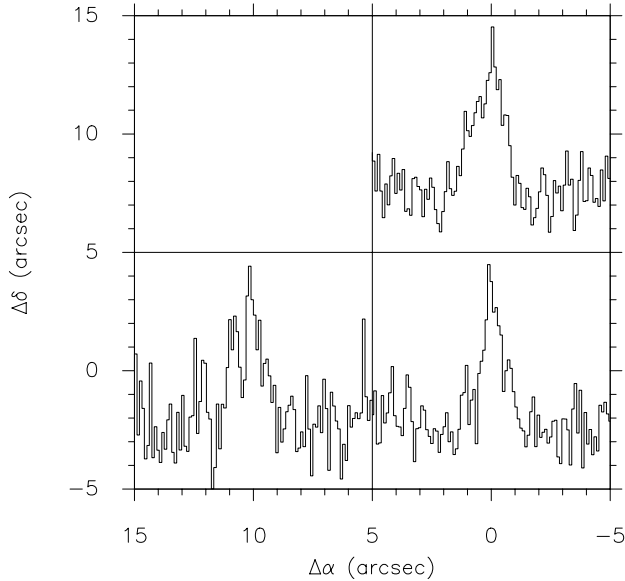


Figure 1. Map of the $J = 1 \rightarrow 0$ spectra of Haro 2. The velocity range is from 1200 to 1700 km s^{-1} . The temperature range is from -0.03 to 0.08 K. Offsets are expressed in arcseconds relative to the position listed in Tab. 1.

a short description of the galaxies as they appear on the Digitized Sky Survey (DSS).

3.1 Haro 2

Haro 2 is a relatively well studied BCDG. Its metallicity is about $\frac{1}{3}$ solar. It has the shape and the brightness profiles of an elliptical galaxy, but possesses a brilliant blue nucleus which shows intense star formation. The absolute blue magnitude is $M_B = -18.^m4$ (Loose & Thuan, 1986). A comparison between the UV, optical and FIR spectra of Haro 2 with evolutionary population synthesis models has allowed to estimate the age of the youngest star formation episode to be 4 million years, followed by two older bursts, the younger of which was over 20 million years ago.

Our CO observations confirm the previous detection of CO in both the $J = 1 \rightarrow 0$ and $J = 2 \rightarrow 1$ transitions by SSLH and by Knapp & Rupen (1996) in the latter transition. The emission is clearly extended, as seen in Fig. 1, with significant lines in all positions (see Tab. 3). Moreover, Fig. 2 suggests that the line in Haro 2 has two components which are seen at the same velocities in both transitions. Recently, observations with the IRAM interferometer fully confirmed this finding (Fritz et al., in prep.). The line ratio of the $(2 \rightarrow 1)$ to the $(1 \rightarrow 0)$ line seems to be independent of the velocity (see Fig. 2). Following the path of SSLH, we calculate two extreme line ratios, one assuming the source to be point-like, and one assuming a uniformly filled beam. In the latter case, since a beam filling factor of 1 is assumed, the ratio of the lines is effectively the ratio of integrated lines. This is also true if the filling factor is < 1 , but equal for both transitions (i.e. in the presence of large scale clumping). For a point source the other extreme is considered: one assumes that the $(2-1)/(1-0)$ intensity ratio is overestimated by exactly the ratio of the two beam areas, so that the

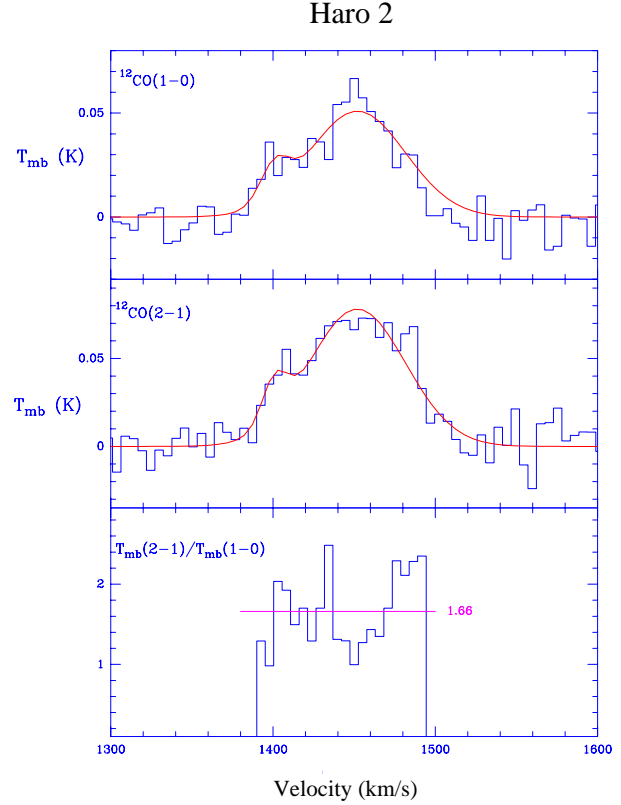


Figure 2. Average spectra and line ratio of Haro 2. The presence of two components of the line is suggested, but it is not reflected by a change of the line ratio.

maximum line ratio must be divided by the ratio of the squares of the two beam widths ($\simeq 3.1$). The results are shown in Table 4 and range from 0.5 to 1.5. The differences between our ratios and those of SSLH might be partly due to different main beam efficiencies used for the two transitions (not specified by SSLH).

3.2 UM 422

The dominant HII region of this dwarf galaxy is embedded in an extended faint irregular stellar body. We have obtained 5 independent spectra; none of them shows significant CO emission. UM 422 has also been observed with a single pointing by TKS using the NRAO 12m telescope. We confirm their non-detection with a significantly lower upper limit.

3.3 UM 439

In the optical, UM 439 has a slightly elongated compact appearance with one prominent HII region south of the center. High resolution HI observations by van Zee, Skillman & Salzer (1998) reveal that the star formation is taking place in the peak of the extended gas distribution. It was observed in CO by SSLH and by Gondhalekar et al. (1998). We confirm their non-detections. Our upper limit to I_{CO} is a factor of 2.4 lower than that of SSLH obtained with the NRAO 12m telescope and a factor of 2.5 lower than

that obtained with the Onsala 20 m telescope. Because we additionally observed 4 independent positions with higher angular resolution than those just mentioned, our upper limit to L_{CO} is significantly lower than those previously published.

3.4 UM 446

The stellar component of this galaxy, as detected in optical imaging, is very faint. We have observed it only in the central position. Our upper limit for CO is the first one ever published.

3.5 UM 452

We have observed this galaxy towards one position only, where the optical emission is strongest. The optical extent of the galaxy looks much smaller as compared to the HI. The mass of HI is quite low, $M_{\text{HI}} = 5 \times 10^7 M_{\odot}$ (Martin, 1999).

3.6 UM 456

The star forming regions in this galaxy are confined to the center of an extended and distorted stellar component. Taylor et al. (1995) have detected two companions of UM 456. UM 456 A seems to be a pure “HI cloud” with no optical counterpart, whereas UM 456 B is seen both in HI and on optical images. Both companions seem to be gravitationally bound to UM 456. None of them shows CO; with our better rms we do not confirm the “marginal detection” of UM 456 by SSLH; our upper limit is a factor of 6 lower than their claimed detection.

3.7 UM 462

The two BCDGs UM 461 and UM 462 seem to form a bound system with a linear separation of about 70 kpc at a distance of 13.9 Mpc. Two centrally located knots of star formation dominate the optical image of UM 462. They are associated with the peak of the HI column density (Van Zee et al., 1998). The claimed detection of CO in UM 462 by SSLH could not be confirmed; our upper limit is a factor of 2 lower. This galaxy had also been observed by Gondhalekar et al. (1998) with a higher upper limit obtained at lower angular resolution.

3.8 UM 465

The optical appearance of this dwarf galaxy is circular in shape with an exponential law brightness distribution (Doublier et al, 1997). The nuclear starburst and extended dust lanes and patches are well resolved by HST imaging (Malkan et al., 1998). A faint nearby object was not detected in HI (Taylor et al., 1995) but confirmed as a physical neighbour (Doublier et al, 1997) using 6 m telescope spectroscopy. The HST images of this companion reveal an irregular structure. While SSLH reported a marginal detection in UM 465 of CO, the present work delivers a clear one. The CO emission is extended in this galaxy (see Fig. 3), but with a lower intensity than Haro 2. Only in one of

Table 4. Comparison of the line intensity ratios of Haro 2 and UM 465, calculated for different filling factors.

Source	Point source $\frac{2 \rightarrow 1}{1 \rightarrow 0}$	Uniform filling $\frac{2 \rightarrow 1}{1 \rightarrow 0}$	Reference
Haro 2	0.31 ± 0.04	1.0 ± 0.1	SSLH
	0.49 ± 0.03	1.51 ± 0.07	this work ^a
UM 465	0.27 ± 0.11	0.91 ± 0.36	SSLH
	0.42 ± 0.11	1.30 ± 0.35	this work

Remarks: The errors are derived formal errors of the fits. *a*: The two components have been averaged.

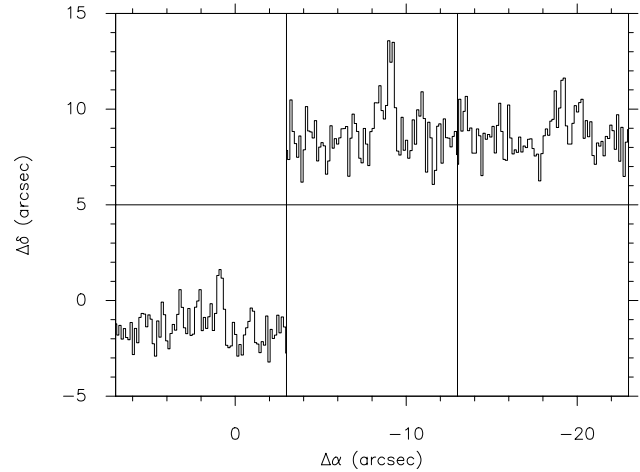


Figure 3. Map of the $J = 1 \rightarrow 0$ spectra of UM 465. The velocity range is from 900 to 1300 km s^{-1} . The temperatures range from -0.02 to 0.04 K. Offsets are expressed in arcseconds relative to position given in Tab. 1

the three positions no $J = 2 \rightarrow 1$ line was detected. The calculated line ratios are listed in Table 4, and for this galaxy they range between 0.4 and 1.3.

4 DISCUSSION

Our deep observations corroborate the difficulty to detect CO in BCDGs. Only two of the galaxies observed show significant CO emission; in both cases it is extended in both transitions. We note here that these two sources are those with the highest metallicity in our sample. In the other sources, even with observations towards several positions, we were unable to find CO emission. One could be tempted to say that these galaxies are void of molecular gas, but this conclusion is premature because the relationship of CO emission and H_2 content in a galaxy depends on many factors (Maloney & Black (1988), Israel (1997)), some of which are not fully understood. Therefore, one can only conclude from the detection of CO that H_2 is present, whereas the absence of CO does not necessarily imply a lack of H_2 .

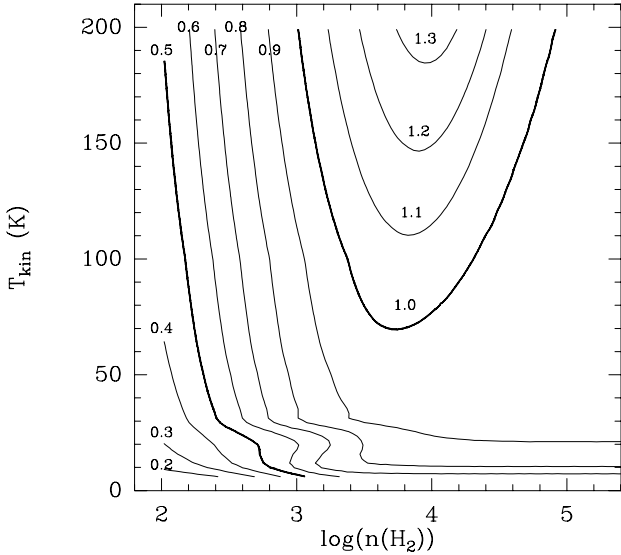


Figure 4. Line intensity ratios as calculated with a LVG code. Solid lines represent $\mathcal{R}_{2/1}$, which is the predicted ratio between the $2 \rightarrow 1$ and the $1 \rightarrow 0$ lines. A velocity gradient of $1 \text{ km s}^{-1} \text{ pc}^{-1}$ and $[\text{CO}/\text{H}_2] = 2 \cdot 10^{-5}$ have been assumed. Contour values are given in the figure.

4.1 Physical conditions of the gas

As a first step in our analysis, we try to infer some information on the physical properties of the CO-emitting gas in BCDGs. We make use of a large velocity gradient (LVG) model to predict ratios for the lowest CO lines. The basic LVG assumption is that of a systematic monotonic velocity gradient, which allows to treat the molecular excitation as a local problem (see de Jong, Chu & Dalgarno, (1975) and White (1977) for details). This is certainly an idealization of extra-galactic cloud complexes; however, an LVG code does not require detailed knowledge of the velocity field. As a first rough estimate this model further assumes constant density and kinetic temperature within the molecular cloud. In Fig. 4, we show an example of the dependence of line ratios on $n(\text{H}_2)$ and T_{kin} . For this figure, $\frac{[\text{CO}/\text{H}_2]}{|\nabla v|} = 2 \cdot 10^{-5} \text{ (km s}^{-1} \text{ pc}^{-1})^{-1}$ has been assumed. This corresponds to a velocity gradient of $1 \text{ km s}^{-1} \text{ pc}^{-1}$ and an abundance of $[\text{CO}/\text{H}_2] = 2 \cdot 10^{-5}$ or, due to how the LVG code is constructed, to a velocity gradient of $5 \text{ km s}^{-1} \text{ pc}^{-1}$ and $[\text{CO}/\text{H}_2] = 10^{-4}$. The figure shows the ratios of the intensities of the $2 \rightarrow 1$ to $1 \rightarrow 0$ transitions, $\mathcal{R}_{2/1}$, and that of $3 \rightarrow 2$ and the $2 \rightarrow 1$ lines, $\mathcal{R}_{3/2}$.

As discussed above, for Haro 2 and UM 465 the line ratios are $0.49 \leq \mathcal{R}_{2/1} \leq 1.51$ and $0.42 \leq \mathcal{R}_{2/1} \leq 1.30$, respectively, depending on the filling of the sources in our beam. From our limited mapping of the two galaxies, we know that the sources are extended and the “point source” limit can be firmly excluded. On the other hand, observations of Haro 2 obtained with the Plateau de Bure Interferometer (Fritz et al., in prep.) show that the galaxy does not fill the beam of the IRAM 30 m telescope uniformly. It is then reasonable to expect a value for the line intensity ratios in between those listed in Table 4, and may thus be close to unity.

Adopting a ratio $\mathcal{R}_{2/1}$ between 0.8 and 1.0, we can

derive from Fig. 4 that the gas is either at high temperatures with medium densities (\approx a few hundred cm^{-3}) or at high densities ($\geq 2000 \text{ cm}^{-3}$) and low temperatures ($T_{\text{kin}} \leq 50 \text{ K}$). More stringent limits on volume density and kinetic temperatures require observations of higher ^{12}CO transitions and/or ^{13}CO transitions. These transitions are expected to be very weak though, and thus difficult and time-consuming.

4.2 Dependence of the CO luminosity on metallicity and absolute blue magnitude

We subsequently examine the relation of the CO emission and metallicity. Because only the two galaxies in our sample with the highest metallicities are detected in CO, one could expect that CO luminosity depends on metallicity. Therefore, we plot our CO luminosities (L_{CO}) – listed in Table 1 – vs. the metallicities of the galaxies of our sample. Since not all of the galaxies have known metallicities, we are left with only 6 galaxies. These are shown in Fig. 5. In this figure we also include the data points given by TKS because they represent the most comprehensive sample of CO observations of dwarf galaxies with metallicity determinations. We only selected those dwarf galaxies from the sample with metallicities better determined than 0.1 dex; these galaxies are, however, not necessarily classical BCDGs.

We have chosen the CO luminosity because it is largely independent of distance, although the error in the distance determination enters as the square in the CO luminosity. Furthermore, the CO luminosity is directly proportional to the H_2 mass corrected for helium ($M(\text{H}_2) = 2.2 \cdot X_{\text{CO}} \cdot L_{\text{CO}}$), with M in M_{\odot} and L_{CO} in $\text{K km s}^{-1} \text{ pc}^2$. X_{CO} (in units of $10^{20} \text{ molecules cm}^{-2} (\text{K km s}^{-1})^{-1}$) is the well-known but poorly determined X_{CO} factor which relates the molecular hydrogen column density to the observed integrated CO line intensity ($X_{\text{CO}} \equiv N(\text{H}_2)/I_{\text{CO}}$).

Fig. 5 shows a general trend that galaxies with higher metallicities have higher CO luminosities, although no functional correlation is visible. TKS have recently proposed that galaxies with metallicities below 7.9 are basically undetectable in CO. Our data do not contradict this finding. For galaxies close to that limit we were only able to derive upper limits. We note, however, that even above that limit there are galaxies not detected in CO.

Although it is qualitatively expected that a higher metallicity leads to a higher L_{CO} because of the availability of the building blocks of the CO molecule, Fig. 5 shows that the oxygen abundance cannot be the only factor influencing the CO luminosity. Because BCDGs are actively star-forming galaxies, the UV radiation field may be locally high. This plays two conflicting roles for CO: on the one hand, it heats the gas, so that the excitation temperature is higher and CO is brighter; on the other hand, if hard enough, it destroys CO via photodissociation, thus the CO emission becomes weaker. Pak et al. (1998) and Bolatto, Jackson & Ingalls (1999) have studied these effects and found that the CO emitting regions are effectively smaller in low-metallicity environments and most of the carbon is present in atomic form. The net effect in galaxies with low metallicities is that, due to low beam filling of the clouds, the molecular gas becomes invisible in the CO lines and might be better

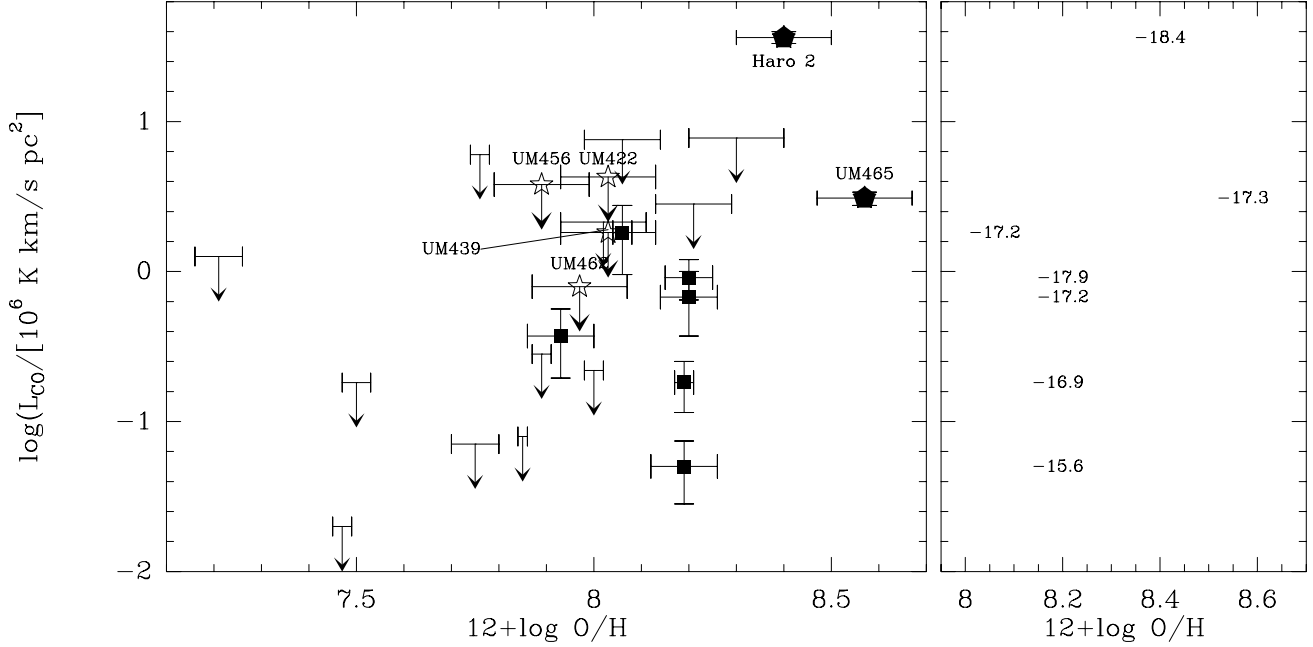


Figure 5. Dependence of the CO luminosity on the metallicity of dwarf galaxies. Our non-detections are marked as open stars, detections as filled diamonds. Detections from the compilation of TKS are marked as filled squares. Arrows mark upper limits. On the left side of the plot all galaxies are shown. On the right side only galaxies with a well determined CO luminosity are shown. Here the numbers represent the absolute blue magnitudes of the galaxies.

traced in the fine structure lines of CI and CII. This different beam filling might be the cause for the dependence of the integrated CO line intensity I_{CO} on the metallicity found by TKS.

To study the effect of the radiation field on the CO luminosity, we labelled the values in the CO luminosity-metallicity plane with the absolute blue magnitudes of the galaxies (right side of Fig. 5). Again there is no simple relation between any two of these quantities. However, there is evidence for an influence of both metallicity and absolute blue magnitude on the CO luminosity, meaning that higher blue magnitudes lead to higher CO luminosity for a given metallicity. It also appears that at lower metallicities a higher absolute blue magnitude is necessary to reach a certain CO luminosity. Clearly, more well-observed galaxies are necessary to study the relation between the three quantities.

4.3 Molecular gas masses and the X_{CO} factor

Directly linked to the question of the dependence of the CO luminosity on metallicity and radiation field is the question of which X_{CO} factor is applicable to low-metallicity galaxies. A number of studies have examined possible correlations between X_{CO} and the metallicity (e.g. Dettmar & Heithausen (1989), Wilson (1995), Verter & Hodge (1995), Arimoto, Sofue & Tsujimoto (1996)). Klein (1999) has proposed an additional dependence of X_{CO} on the cosmic ray flux as judged from the radio continuum brightness.

An independent determination of the X_{CO} factor for our BCDG sample would be useful to determine their molecular masses; this is, however, beyond the scope of this paper. A

Table 5. Molecular masses from predicted X_{CO} factors.

Source	X_{CO}	$M(H_2)$ $10^8 M_\odot$	$M(HI)$ $10^8 M_\odot$
UM 422	18.6	≤ 1.3	26
UM 439	18.6	≤ 0.6	3.5
UM 456	25.7	≤ 1.6	3.7
UM 462	21.4	≤ 0.3	2.9
UM 465	5.4	0.3	0.39
Haro 2	7.9	4.7	4.8

Remarks: X_{CO} factors are derived from the metallicity dependence as given by Arimoto et al. (1996), using metallicities from Table 1. X_{CO} is given in units of 10^{20} molecules cm^{-2} $(K km s^{-1})^{-1}$. HI masses for UM galaxies are from Taylor et al. (1995), for Haro 2 from SSLH.

reliable value for X_{CO} has been established for the disk of the Milky Way, X_{MW} . The currently best accepted value is $X_{MW} = 1.6 \cdot 10^{20}$ molecules $cm^{-2} K^{-1} km s^{-1}$ (Hunter et al., 1997). X_{CO} factors determined for galaxies with lower metallicities are usually significantly higher (e.g. Cohen et al. (1988), Dettmar & Heithausen (1989)).

In the following, we assume that the correlation between X_{CO} , derived from a virialization analysis of several galaxies, and the oxygen abundance obtained by Arimoto et al. (1996) gives X_{CO} factors applicable to our galaxy sample. H_2 masses derived under this assumption are listed in Table 5. Also given are the HI masses as derived by (Taylor et al., 1995) for the UM galaxies and by SSLH for Haro 2. One remarkable result from this calculation is that those galaxies undetected in CO have upper limits on the molecular gas mass significantly below the HI mass, whereas in the two

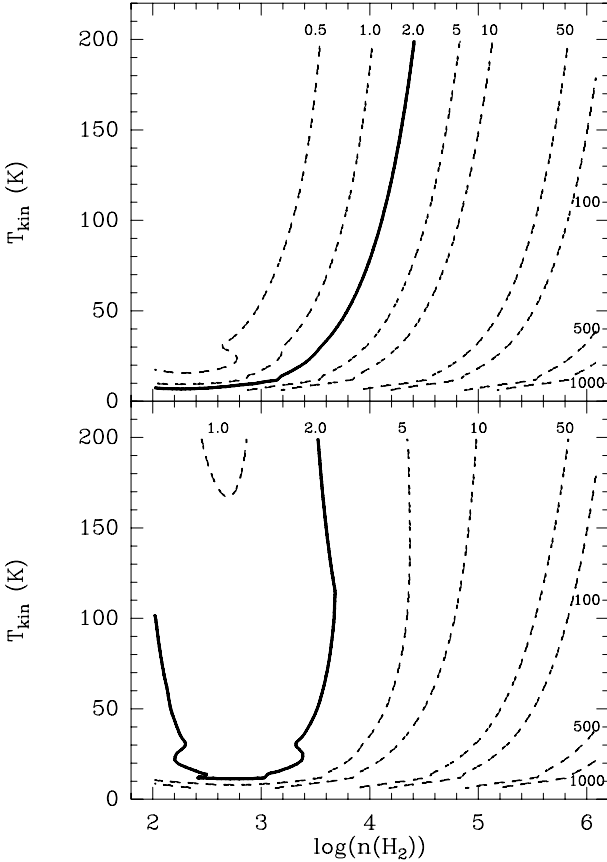


Figure 6. The variation of X_{CO} with changing kinetic temperature and volume density, as derived from the LVG approximation. Values at the contours give X_{CO} in units of $10^{20} \text{ cm}^{-2} (\text{K km s}^{-1})^{-1}$. The velocity gradient is fixed to $2 \text{ km s}^{-1} \text{ pc}^{-1}$. In the top panel, the abundance is $[\text{CO}/\text{H}_2] = 10^{-4}$; in the bottom panel $[\text{CO}/\text{H}_2] = 10^{-5}$, two values between which it is likely to find most BCDGs. The thick solid lines represent the value for the Milky Way, $X_{\text{MW}} \sim 2 \cdot 10^{20} \text{ cm}^{-2} (\text{K km s}^{-1})^{-1}$.

galaxies where CO is detected, HI and H_2 masses are about the same.

The X_{CO} factors used here to derive molecular gas masses are *global* factors. Studying the CO emission of the Magellanic Clouds with different angular resolutions Rubio, Lequeux & Boulanger (1993) noted that the derived X_{CO} factor depends on the linear resolution, implying that the *local* X_{CO} value is lower than the *global* one.

In order to calculate the *local* X_{CO} we use an LVG approximation assuming that H_2 and CO share the same volume. The LVG approximation can then be used to derive the H_2 column density, $N(\text{H}_2)$, from $N(\text{H}_2) = n(\text{H}_2) \Delta v / |\nabla \vec{v}|$, where $n(\text{H}_2)$ is the H_2 volume density, Δv is the line width and $|\nabla \vec{v}|$ is the velocity gradient. Since $I_{\text{CO}} \simeq T_{\text{mb}} \Delta v$, one can derive X_{CO} from $X_{\text{CO}} = N(\text{H}_2) / I_{\text{CO}} \propto n(\text{H}_2) / |\nabla \vec{v}| T_{\text{mb}}$.

The dependence of the local X_{CO} on varying volume density and kinetic temperature is shown in Fig. 6. The velocity gradient is fixed to $2 \text{ km s}^{-1} \text{ pc}^{-1}$. In the top panel, the abundance is $[\text{CO}/\text{H}_2] = 10^{-4}$; in the bottom panel $[\text{CO}/\text{H}_2] = 10^{-5}$. These are extreme values for the metallicities of BCDGs. X_{MW} is indicated by the thick solid line. We note that, once the density becomes high enough,

X_{CO} will not change significantly any more, due to the growth of the optical depth, and X_{CO} is independent of the abundance. On the other hand, at lower densities and kinetic temperatures, X_{CO} changes significantly depending on $n(\text{H}_2)$ and T_{kin} for a given metallicity.

These simple calculations indicate that X_{CO} does not only depend on the metallicity of a galaxy. Physical parameters, such as average volume density and kinetic temperature, play important roles, if the density is below 10^4 cm^{-3} and/or the kinetic temperature is below 50 K, values found in many molecular clouds in the Milky Way. The X_{CO} -factor, that we find for a standard density of 10^3 cm^{-3} and a low-metallicity environment, is low, i.e. close to Galactic. In contrast, X_{CO} derived from the formula of Arimoto et al. (1996) is higher by an order of magnitude. This supports the concept of large amounts of hidden gas - either atomic or molecular.

Interferometric observations of BCDGs might help to resolve this issue. Such a study of the nearby post-starburst dwarf NGC 1569, a galaxy that may be considered as a nearby BCDG in a post-starburst phase, yielded a rather high value of $X_{\text{CO}} = 6.6 \cdot X_{\text{MW}}$, based on virial masses of resolved GMCs (Taylor et al., 1999). This indicates that this method, which is also the basis of Arimoto’s formula, is sensitive to the ‘hidden’ H_2 and tends to yield global values for X_{CO} . In contrast, we expect to find local values if line ratio studies encompassing several CO isotopomers become available, since these studies directly probe the physics of the gas from which the CO emission arises.

5 CONCLUSIONS

We have searched for emission from the ^{12}CO ($J = 1 \rightarrow 0$ and $J = 2 \rightarrow 1$) transitions in 10 dwarf galaxies, 8 of which are BCDGs and 2 are the companions of one of these. We detected CO in 2 of them (Haro 2 and UM 465) and found it to be extended in both galaxies. Although we mapped part of the other galaxies, we were unable to detect CO. We obtained very stringent upper limits. We could not confirm the “marginal detection” of CO in UM 456 and UM 462 previously reported by SSLH.

The observed line ratios of the $2 \rightarrow 1$ to $1 \rightarrow 0$ transitions are not very sensitive to changes in the kinetic temperature. Modelling the ratio with a simple LVG code helps only to exclude low densities. Higher CO transitions and/or observations of CO isotopomers will help to get more stringent limits on these physical parameters.

We could not find any simple relation between metallicity and CO luminosity. Molecular gas masses for the galaxies are derived assuming the relation between X_{CO} and metallicity given by (Arimoto et al., 1996). We find that for those galaxies detected in the CO lines the molecular gas mass is comparable to the HI mass, whereas for those galaxies undetected in CO the HI mass is significantly larger than the limits on the molecular gas mass.

Even in the sources where CO has not been detected, we do not argue against the presence of H_2 . While it is certainly possible that in the extreme environment of a BCDG not just CO but also H_2 is destroyed, at least in regions close to young massive stellar clusters, a picture in which a large amount of H_2 exists without CO is attractive. Sensitive

observations of CI and CII in these galaxies would thus be desirable in the future to shed light on this issue.

ACKNOWLEDGEMENTS

L.T.B. would like to thank Prof. Loretta Gregorini and the Socrates/Erasmus project which made this exchange possible and financed it, the Faculty of Science of the University of Bologna and the C.N.A.A. (*Consorzio Nazionale per l'Astronomia e l'Astrofisica*) for grants supporting this work. This project was supported by the Deutsche Forschungsgemeinschaft via the Graduiertenkolleg “*The Magellanic Clouds and other Dwarf Galaxies*”.

REFERENCES

- Arimoto N., Sofue Y., Tsujimoto T., 1996, PASJ 48, 275
 Arnault P., Casoli F., Combes F., Kunth D., 1988, A&A 205, 41
 Barone L.T., 1998, Tesi di Laurea, Università degli Studi di Bologna.
 Bolatto A.D., Jackson J.M., Ingalls J.G., 1999, AJ 113, 275
 Brinks E. 1990, in *Dynamics and Interaction of Galaxies*, Ed. R. Wielen, Springer Verlag, Berlin, p. 146
 Campos-Aguilar A., Moles M., Masegosa J., 1993, AJ 106, 1784
 Cohen R.S., Dame T.M., Garay G., Montani J., Rubio M., Thaddeus P., 1988, ApJ 331, L95
 de Jong T., Chu S.L., Dalgarno A., 1975, ApJS 19, 69
 Dettmar R.J., Heithausen A., 1989, ApJ 344, L61
 Doublier V., Comte G., Petrosian A., Surace C., Turatto M., 1997, A&AS 124, 405
 Gondhalekar P.M., Johansson L.E.B., Brosch N., Glass I.S., Brinks E., 1998, A&A 335, 152
 Hunter S.D., Bertsch D.L., Catelli J.R., et al., 1997, ApJ, 481, 205
 Israel F.P., 1997, A&A 328, 471
 Klein U.: 1999, *Molecular gas in dwarf galaxies*. In: XVIII Moriond Astrophysics Meeting (14-21 March 1998), *Dwarf galaxies and Cosmology*, Thuan T.X., Balkowski C., Cayatte V., Van J.T.T. (eds.), In press.
 Knapp G.R., Rupen M.P., 1996, ApJ 460, 271
 Kunth D., Östlin G., 2000, A&AR (in press)
 Loose, H.-H., Thuan, T.X., 1986, ApJ 309, 59
 Malkan M.A., Gorjian V., Tam R., 1998, ApJS 117, 25
 Maloney P., Black J.H., 1988, ApJ 325, 389
 Martín M.C., 1999, A&A 131, 77
 Pak S., Jaffe D.T., van Dishoeck E.F., Johansson L.E.B., Booth R.S., 1998, ApJ 498, 735
 Rubio M., Lequeux J., Boulanger F., 1993, A&A 271, 9
 Sage L.J., Salzer J.J., Loose H.-H., Henkel C., 1992, A&A 265, 19 (SSLH)
 Salzer J.J., 1989, ApJ 347, 152
 Sargent W.L.W., Searle, L., 1970, ApJ 162, L155
 Searle L., Sargent W.L.W., 1972, ApJ 173, 25
 Tacconi, L.J., Young J.S., 1984, ApJ 290, 602
 Taylor C.L., Brinks E., Grashuis R.M., Skillman E.D., 1995, ApJS 99, 427
 Taylor C.L., Kobulnicky H.A., Skillman E.D., 1998, AJ 116, 2746 (TKS)
 Taylor C.L., Hüttemeister S., Klein U., Greve A., 1999, A&A 349, 424
 Thuan, T.X., 1983, ApJ 268, 667
 Thuan, T.X., Martin, G.E., 1981, ApJ 247, 823
 Verter F., Hodge P., 1995, ApJ 446, 616
 White R.F., 1977, ApJ 211, 744
 Wilson C.D., 1995, ApJ 448, L97

van Zee L., Skillman E.D., Salzer J.J., 1998, AJ 116, 1186

This paper has been produced using the Royal Astronomical Society/Blackwell Science L^AT_EX style file.